The Effect of Basicity on the Radiative Heat Transfer and Interfacial Thermal Resistance in Continuous Casting

KEZHUAN GU, WANLIN WANG, LEJUN ZHOU, FANJUN MA, and DAOYUAN HUANG

The basicity of mold flux has been recognized to have a significant influence on the mold flux crystallization in continuous casting, which would in turn affect the heat-transfer rate between the solidified shell and mold. The research regarding the mold flux crystallization as well as its effect on the heat transfer has been conducted intensively. However, few studies have been developed to specify the effect of basicity introduced mold flux crystallization on the radiative heat transfer and interfacial thermal resistance in continuous casting. By using an infrared radiation emitter, a radiative heat flux was applied to a copper mold covered with a solid mold flux disk to simulate the heat-transfer phenomena in continuous casting. The crystallization behaviors of mold fluxes with different basicities and their impact on the radiative heat transfer were investigated dynamically. The interfacial thermal resistance between the solid mold flux and copper mold was also studied in this article. The results suggested that the basicity tends to enhance the mold flux crystallization, leading to the reduction of radiative heat-transfer rate and enlargement of interfacial thermal resistance.

DOI: 10.1007/s11663-012-9644-4

I. INTRODUCTION

AS the surface of final slabs is influenced strongly by the heat-transfer rate during the initial solidification of the molten steel, many studies have been carried out to investigate the heat-transfer phenomenon between the strand and mold.[1–5] The traditional casting parameters, such as casting speed, oscillation frequency, steel compositions, and the properties of casting powder have been studied and recognized as the major factors in regulating the heat-transfer rate.[6–10] Among all these factors, mold flux infiltration between the mold and strand that introduces thermal resistances to the conductive and radiative heat transfers is used generally to moderate the heat-transfer rate to prevent the occurrence of surface defects on continuously cast steel slabs.

The mold flux between the stand and mold is composed usually of three layers depending on the cooling rate, *i.e.*, a solid glassy layer against the mold wall resulting from the large cooling rates during the initial contact of the molten slag with the water-cooled cooper mold,[11] a precipitated crystalline layer in the center, and a molten film in contact with the steel strand. Previous studies could be referred to for the detailed schematic heat-transfer phenomena across deferent layers.[12] It has been acknowledged that the precipitation of crystals in mold flux film can decrease the heat-transfer rate, and a lot of research has been conducted to study the reduction of heat transfer caused by the mold flux crystallization,[13,14] and it could be summarized into two categories: those that ascribe the decrease in heat transfer through crystallization as the enlargement of the air gap at the interface between the solid mold flux and copper mold through, *i.e.*, the interfacial thermal resistance,[13,15–17] and those that suggest crystallization lowers the transmissivity of the mold flux through the inferred emitter technique, which in turn reduces the radiative heat flux.[3,18] Some numerical methods[19,20] have also been developed recently to study the interfacial thermal resistance; the typical model like COND1D (SPM Instrument AB, Strängnäs, Sweden) was developed to simulate the temperature evolution in the mold and interface in continuous casting.[21]

Basicity (R), which is usually defined as the ratio of CaO to SiO_2, has been regarded as the most significant effect on the mold flux crystallization. The study by Li *et al.*[22] showed that the addition of CaO caused a dramatic increase in the amount of crystalline phase formed, and it was observed that the increasing basicity could simplify the silicate structure, which will enhance the crystallization process and decrease the viscosity of mold fluxes.[23,24] Similar research conducted at Carnegie Mellon indicated that the added O^{2-} provided by CaO can decrease the degree of polymerization of silicate structures and decrease the viscosity of molten mold flux, which in turn would improve the effective crystallization rate.[25]

As the basicity affects strongly the mold flux crystallization and the mold flux crystallization has a significant effect on the radiative heat transfer and interfacial thermal resistance as suggested, the understanding of how the basicity affects the radiative heat transfer and interfacial thermal resistance in continuous casting

KEZHUAN GU, Graduate Student, WANLIN WANG, Professor, LEJUN ZHOU, Ph.D. Student, and FANJUN MA and DAOYUAN HUANG, Post-Doctors, are with the School of Metallurgical Science and Engineering, Central South University, Changsha 410083, P.R. China. Contact e-mail: wanlin.wang@gmail.com
Manuscript submitted October 25, 2011.
Article published online March 8, 2012.

becomes important. However, little research has been conducted to specify this effect because of the difficulty in determining an exact expression for the radiative heat flux in continuous casting.

In this study, an infrared heat emitter was used to irradiate the surface of a copper mold that was covered with solid glassy mold flux disks with various basicities. Then, the responding in-mold heat flux could be analyzed by the response of the subsurface mold temperatures. The experiments were recorded by a digital camcorder to investigate the crystallization behavior of mold fluxes. Finally, the effect of basicity on the radiative heat transfer and interfacial thermal resistance was studied by analyzing the measured heat fluxes and the recorded images. The detailed mechanisms of radiative heat-transfer model and basic radiation properties of the flux-copper system could be referred as our previous studies.[3,26]

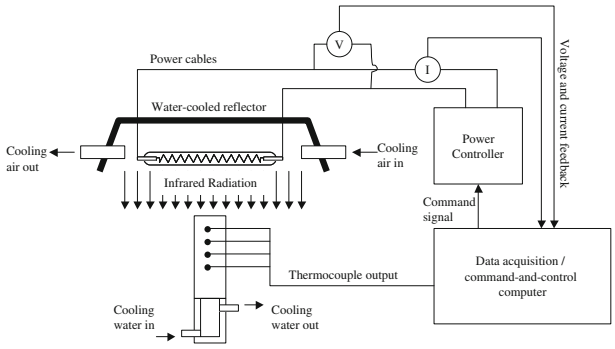

Fig. 1—Schematic illustration of the infrared emitter.

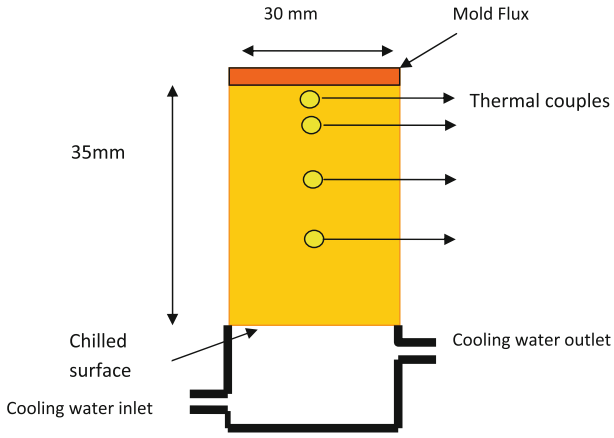

Fig. 2—Schematic figure of copper substrate used as the radiation target.

II. EXPERIMENTAL APPARATUS AND PROCEDURES

A. *Heat-transfer Simulator*

A schematic of the experimental apparatus developed at Central South University (Changsha, China) was shown in Figure 1, the details of which have been described elsewhere.[3] The experimental apparatus mainly included a power controller, an infrared radiant heater capable of emitting 2.0 MW/m^2 heat flux at the rate of 380 voltages, a data-acquisition system, and a command-and-control unit.

The copper mold was simulated by a one-end, water-cooled copper cylinder, which acted as the radiation target, and its schematic figure was shown in Figure 2. As the heat flux was applied to the top surface of the copper mold, which was covered with mold flux disk, the response temperatures could be measured by the subsurface thermocouples.

B. *Mold Flux Disk Preparation*

Four samples with different basicity were studied in this paper, and their main chemical compositions after premelting were listed in Table I. The mold fluxes were decarburized by placing them into a programmable furnace at 1073 K (800 °C) prior to the fusion process. Then, the decarburized flux was melted at 1723 K (1500 °C) in a crucible in an induction furnace for 300 seconds and then quenched from its molten state onto a stainless steel plate at room temperature to achieve a fully glass phase. A new cylindrical, tube-like copper mold with the same diameter as the copper substrate was used to cast the mold flux before it solidified on the steel. The mold flux disks were then polished with the SiC sand papers down to 1200 (grit size) to control its surface roughness and thickness. As reported in our previous study,[27] the evaporative loss of volatile fluoride is not significant, and the premelted chemical composition was analyzed by X-ray fluoroscopy and listed in Table I.

The polished glassy samples with various basicities were then placed on the top of the copper mold individually for heat-transfer experiments.

C. *Experimental Procedure*

Figure 3 shows the heating profile employed in this article. First, the copper system was preheated with a 500 KW/m^2 thermal radiation, and then it was subjected to a constant 800 KW/m^2 thermal radiation. The output thermal energy was increased at a heating rate of 1 KW/m^{2}s.

Table I. The Chemical Compositions of Commercial Mold Fluxes (in Mass Pct)

	CaO	SiO_2	Al_2O_3	MgO	F	Na_2O	Li_2O	Basicity
Flux 1	33.53	42.03	6.81	2.07	5.84	9.18	0.54	0.8
Flux 2	37.75	37.82	6.95	1.86	6.08	9.06	0.48	1.0
Flux 3	39.55	35.98	7.11	1.94	5.93	8.98	0.51	1.1
Flux 4	41.14	34.32	7.08	2.10	5.79	9.12	0.45	1.2

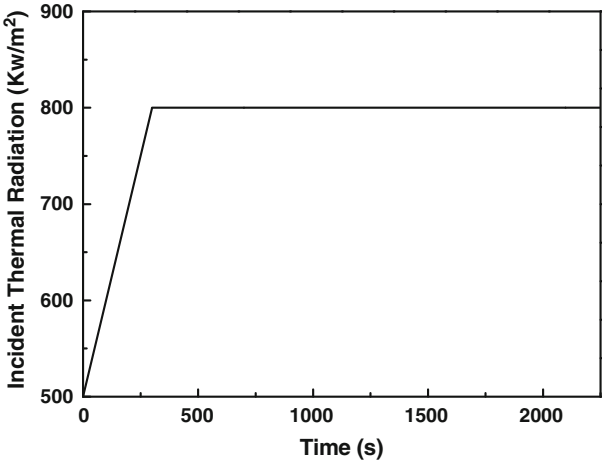

Fig. 3—The heating profile for radiative heat flux measurement.

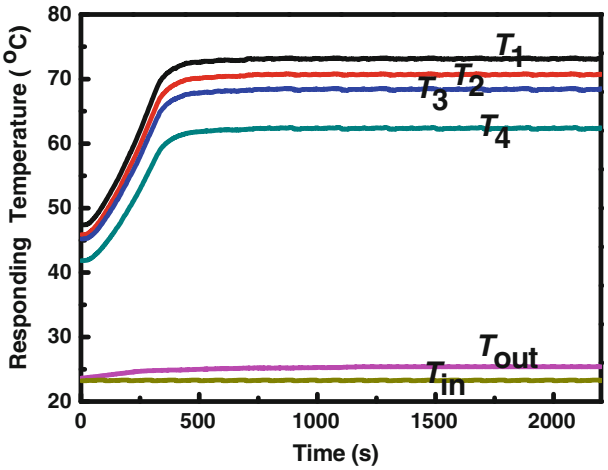

Fig. 4—The in-mold responding temperatures history for bare copper system.

Figure 4 shows the subsurface response temperatures (measured by thermocouples) under a constant 800 KW/m^2 thermal radiation that was irradiated from the infrared emitter to the bare copper mold. The thermocouples placed at 2, 5, 10, and 18 mm below the irradiated surface were recorded as T1, T2, T3, and T4, respectively. The cooling water inlet and outlet temperatures were also recorded as T_{in} and T_{out}. The system reached steady state in 200 to 300 seconds, and the steady-state heat flux q was calculated by Fourier's law

$$q = \frac{-1}{n}\sum_i k\left(\frac{dT}{dx}\right)_i \qquad [1]$$

where n refers to the total number of thermocouples, i is the index number, and $(dT/dx)i$ means the temperature gradient measured by the i^{th} thermocouple. An example of measured heat flux histories for the bare copper system was given in Figure 5, and it could be observed that the measured heat flux was first increased linearly with the addition of the output power, and then it came into a steady state in a short time.

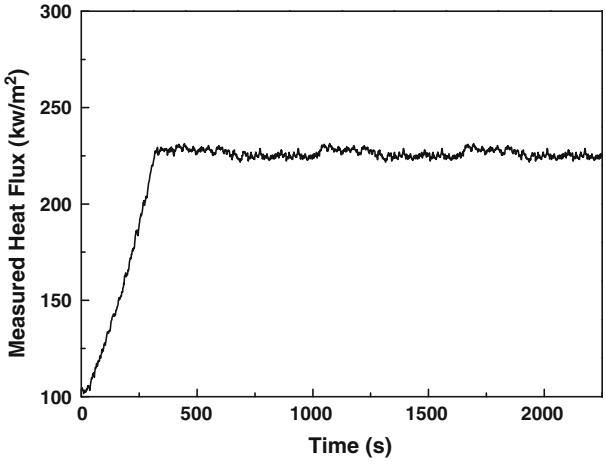

Fig. 5—The measured heat flux history for bare copper system.

III. RESULTS AND DISCUSSION

A. *The In Situ Observation of Responding Heat Fluxes*

Four 3.3-mm-thick glass disks with different basicity as shown in Table I were placed on the copper mold individually and preheated by a 500 KW/m^2 thermal radiation. Then, they were subjected to the thermal heating according to Figure 3. The whole experiment process was recorded by digital camcorder to study the mold flux crystallization behavior.

As the thermal properties in this case are a function of temperature and time, inverse heat conduction estimating the heat flux history for a solid by using measured transient interior temperatures is adapted $\frac{\partial}{\partial x}\left(k\frac{\partial T_i}{\partial x}\right) = \left(\rho c_p\right)\frac{\partial T_i}{\partial t}$, in which ρ is the mass density, c_p is the copper heat capacity, and t is time. Then, by inputting all the thermocouple's temperatures history, the heat flux could be calculated along with the thermal boundary conditions. The heat flux history for the preceding case was calculated and given as the upper line in Figure 6. Four stages appeared in the responding heat flux histories. Stage I was a period in which the heat flux increases linearly with the addition of thermal radiation; stage II is the time from the deviation of the heat flux (as a result of the mold flux crystallization) to its peak value, where the incident energy came to constant; stage III is an attenuation stage where the heat flux continues to reduce under constant radiation as a result of the further crystallization; and stage IV is the period of steady state when the crystallization is completed and the heat flux keeps constant. The images corresponding to each stage were also shown in Figure 6. From those pictures, it was shown clearly that these four disks are fully glassy at stage I, and then the opaque crystals are initiated at the top and developed toward the bottom because of the increasing of thermal radiation at stage II. With a longer annealing time, a higher fraction of glassy disk is crystallized at stage III. Once the system steps into stage IV, there is no further crystallization, and the structure of disks is fixed where the bottom of mold fluxes for $R = 0.8$, 1.0, and 1.1 are keeping glassy, and the one for $R = 1.2$ is crystallized completely.

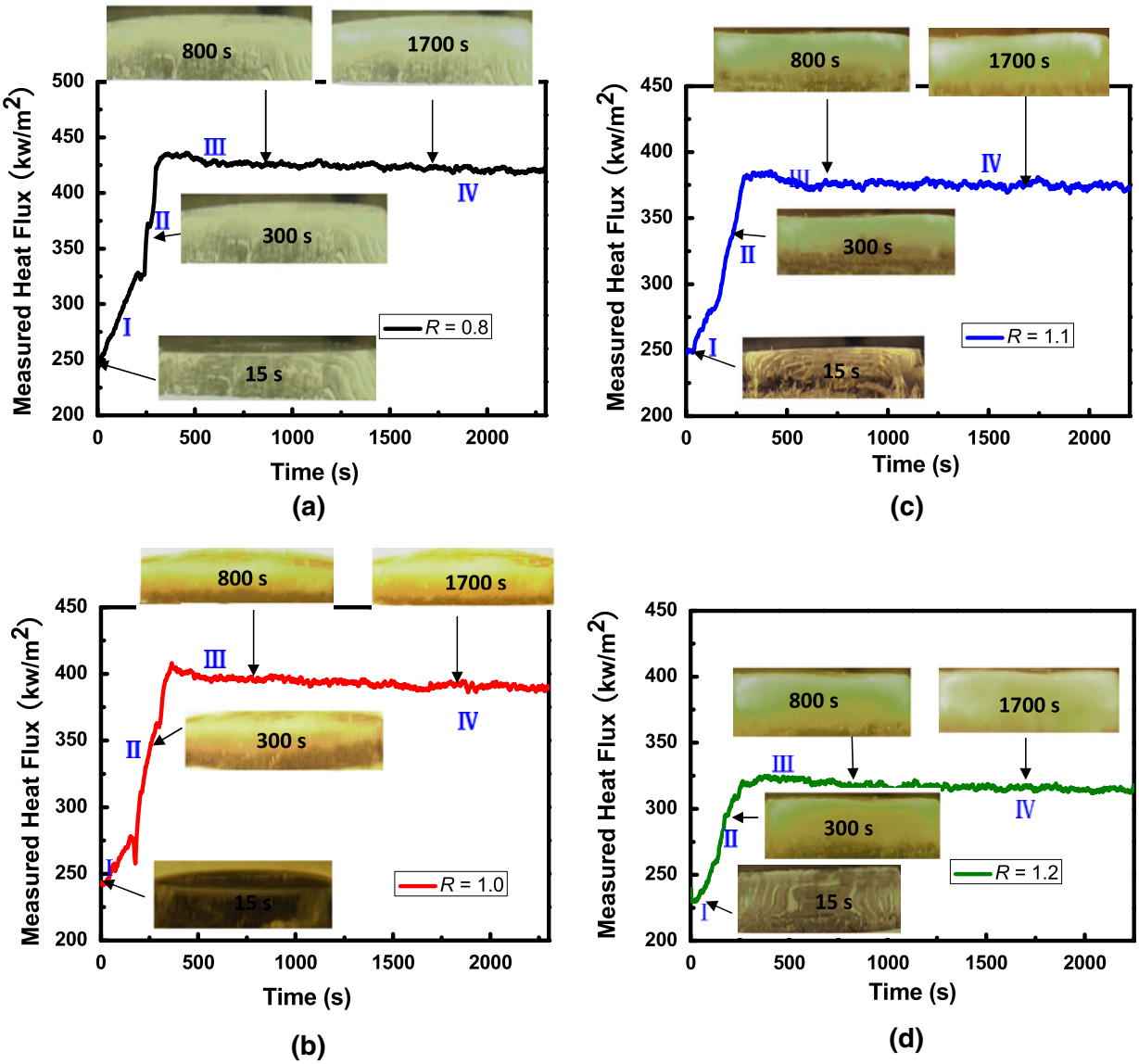

Fig. 6—The measured heat-transfer rates for mold fluxes with various basicities: (*a*) $R = 0.8$, (*b*) $R = 1.0$, (*c*) $R = 1.1$, and (*d*) $R = 1.2$.

B. *Effect of Mold Flux Basicity on Radiative Heat-transfer Rate*

To study the effect of basicity on the radiative heat transfer, the measured heat fluxes and the final cross-section views corresponding to each flux disk were given in Figure 7. It could be observed that the measured heat fluxes at steady state are approximately 423, 391, 378, and 317 KW/m^2 for each individual disk. The steady-state heat flux attenuates from 423 KW/m^2 to 317 KW/m^2 with the increase of the basicity. The thickness of crystalline layer and crystalline fraction for each disk were measured and shown in Figure 8, where the thickness and crystalline fraction are 2.3 mm and 69.8 pct, respectively, when the basicity of slag is 0.8. These two values are increased to 3.3 mm and 100 pct, as the basicity increases to 1.2. Therefore, it could be concluded that the basicity of mold flux does enhance the crystallization of mold flux, which leads to a further crystallization of mold fluxes when they were subjected to same thermal radiation. Consequently, the steady-state heat flux rate decreased with the addition of mold flux basicity because of the increase of crystals fraction

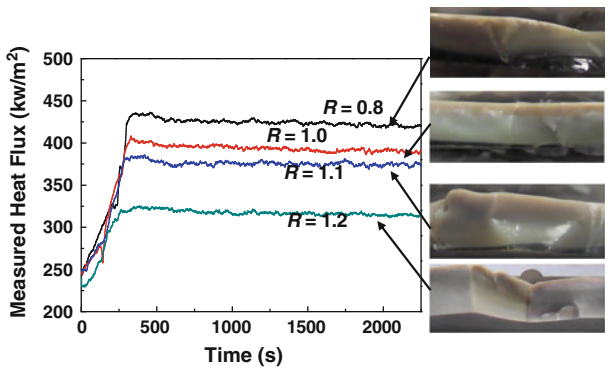

Fig. 7—The measured heat fluxes histories for different mold fluxes.

as shown in Figure 7, as the glassy phase absorbs radiation gradually as it travels through the medium but does not scatter radiation appreciably because of the amorphous structure.[26] However, more incident radiation would be reflected and scattered from the crystals surface, grain boundary, and defects, such that less energy would be absorbed and conducted to the mold.

C. *The Effect of Basicity on Mold Flux Crystallization Behavior*

To study the effect of basicity on the incubation time, the responding heat fluxes during the initial heating period were shown in Figure 9, where the output heating power was increasing from 500 KW/m^2 to 800 KW/m^2 at a rate of 1 KW/m^{2}s.

A clear deviation of the heat flux curve occurred at 215 seconds for disk of $R = 0.8$, 135 seconds for $R = 1.0$, 90 seconds for $R = 1.1$ and 30 seconds for $R = 1.2$. The slag pictures corresponding to each specific time when the heat flux started to deviate were captured and shown in Figure 9, where the opaque crystals were observed clearly at the top of the disks. Therefore, it could be concluded that the deviation of heat flux reflects the beginning of mold flux crystallization because the crystallization retards the heat-transfer rate.

The incubation time and onset crystallization temperature *vs* basicity were plotted in Figure 10. The onset crystallization temperature was measured by the disk top surface temperature T_s, where a thermocouple was placed during the disk fabrication. It could be found that the incubation time of crystallization and the onset crystallization temperature both decrease with the increase of mold flux basicity, which was consistent with our previous study.[27] The incubation time reduces from 215 seconds to 30 seconds when the basicity of mold flux varies from 0.8 to 1.2, and the onset temperature reduces from 1103 K (830 °C) to 951 K (678 °C) as well. The reason for the decrease might be attributed to the fact that CaO is an alkali oxide acting on the silicate network as a network modifier, which could reduce the glass transition temperature and the apparent activation energy of crystal growth by lowering the slag melting temperature and dividing the silicate network in the slag.[28,29]

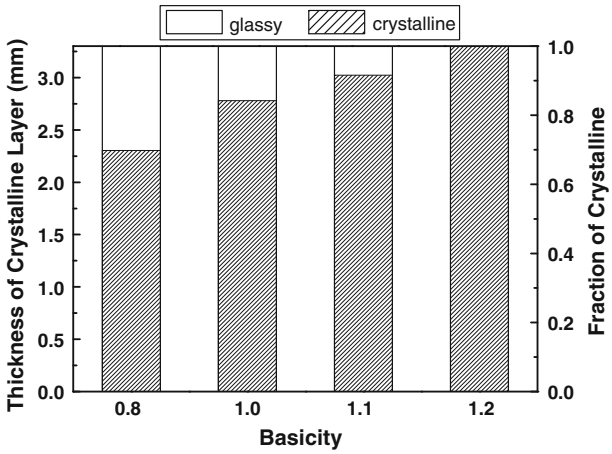

Fig. 8—Thickness of crystalline layer and the crystalline fraction of disks with different basicity.

The measured disk's top surface temperatures T_s first increases with the addition of the heating energy and then starts to fluctuate because of the crystallization of mold flux, and then it steps into the steady state as shown in Figure 11. The steady-state T_s varies from 1144 K (871 °C) to 1435 K (1162 °C), when the basicity changes from 0.8 to 1.2. The reason may be the increased slag thermal resistance that was introduced by the slag disk crystallization, which therefore led to the improvement of disk surface temperature. The larger the crystalline fraction, the higher the surface temperature would be.

D. *Study of the Interfacial Thermal Resistance between the Copper Mold and Mold Flux*

A numerical calculation was conducted to study the effect of mold flux basicity on the interfacial thermal resistance between the copper mold and mold flux. Here, it was assumed that[3,14,30] (1) heat is transferred in one direction from the mold fluxes to the copper mold and (2) the total heat flux is consisted of radiative and conductive heat flux.

Figure 12 shows a schematic temperatures gradient across the mold flux, where T_s represents the top layer of the solid flux temperature as shown in Figure 11, $T_{g/c}$ stands for interfacial temperature between the layer of glassy and crystalline that was determined as the onset crystallization (glass transform) temperature as shown in Figure 10, $T_{s/a}$ is the interface temperature between the bottom surface of solid flux and air gap that was calculated as Eq. [2], and T_m represents the top surface temperature of the copper mold that could be calculated by the in-mold temperature gradient.

$$T_{s/a} = T_m + R_{int} * q_{obs} \quad [2]$$

Therefore, the conductive heat flux across the crystalline and glassy slag layer ($q_{condution}$(crystalline) and $q_{condution}$(glass)) were given by Eqs. [3] and [4].

$$q_{condution}(\text{crystalline}) = K_{crystalline}\frac{T_s - T_{g/c}}{d_{crystalline}} \quad [3]$$

$$q_{condution}(\text{glass}) = K_{glass}\frac{T_{g/c} - T_{s/a}}{d_{glass}} \quad [4]$$

where $K_{crystalline}$ and K_{glass} are the thermal conductivities of the crystalline and glassy mold flux, and $d_{crystalline}$ and d_{glass} are the thickness of the crystalline and glass layer, respectively. The thermal conductivities $K_{crystalline}$ and K_{glass} have been measured by Ozawa *et al.*[31] using the hot wire method, who measured the commercial mold fluxes with the basicity within 0.8 to 1.5, and the main chemical compositions of slags used in the measurements were similar to the ones used in this article. The values were reported as 1.0 to 1.2 W m^{-1} K^{-1} for glassy

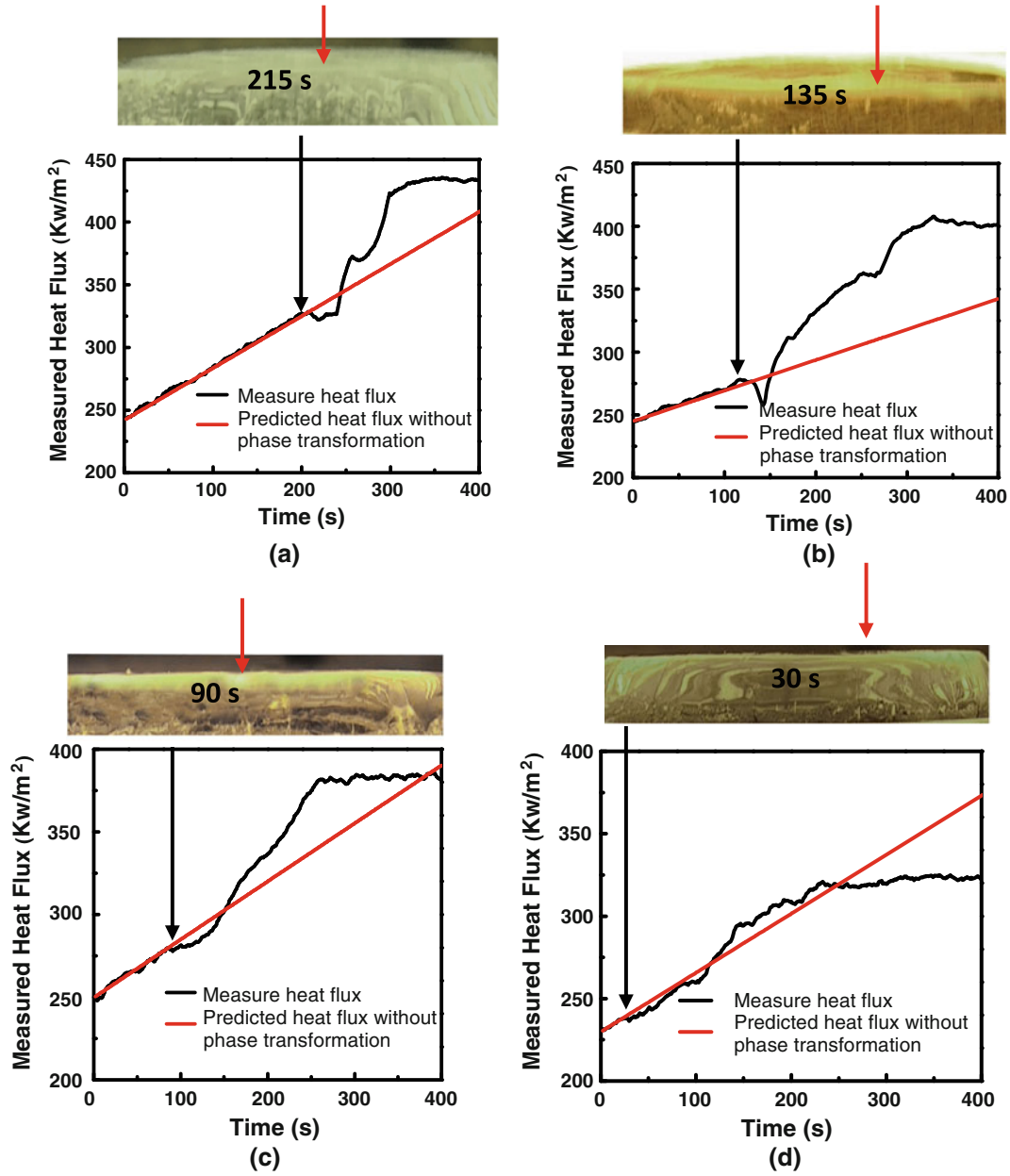

Fig. 9—The measured heat fluxes for the four mold fluxes systems during the initial heating period: (*a*) $R = 0.8$, (*b*) $R = 1.0$, (*c*) $R = 1.1$, and (*d*) $R = 1.2$.

flux film and 1.6 to 1.8 W m^{-1} K^{-1} for the crystalline layer. Radiative heat flux across the crystalline and glassy slag layer ($q_{radiation}$(crystalline) and $q_{radiation}$(glass)) were expressed by the following equations, which has also been employed by other researchers[19,20]:

$$q_{radiation}(\text{crystalline}) = \frac{n^2\sigma}{0.75\alpha_{crystalline}d_{crystalline} + \varepsilon_{crystalline}^{-1} + \varepsilon_{glass}^{-1} - 1} \times \left(T_s^4 - T_{g/c}^4\right) \quad [5]$$

$$q_{radiation}(\text{glass}) = \frac{n^2\sigma}{0.75\alpha_{glass}d_{glass} + \varepsilon_{crystalline}^{-1} + \varepsilon_{mold}^{-1} - 1} \times \left(T_{g/c}^4 - T_{s/a}^4\right) \quad [6]$$

where n is the refractive index that is referred to be 1.6; σ (which is the Stefan-Boltzmann constant) is 5.6705×10^{-8} (W/(m^2K^4); ε represents the emissivity 0.92 for glass, 0.7 for the crystalline mold flux, and 0.4 for the copper mold individually;[32] and α is the absorption coefficient of solid mold fluxes: 400 m^{-1} for glass and 4500 m^{-1} for crystal.[26,33]

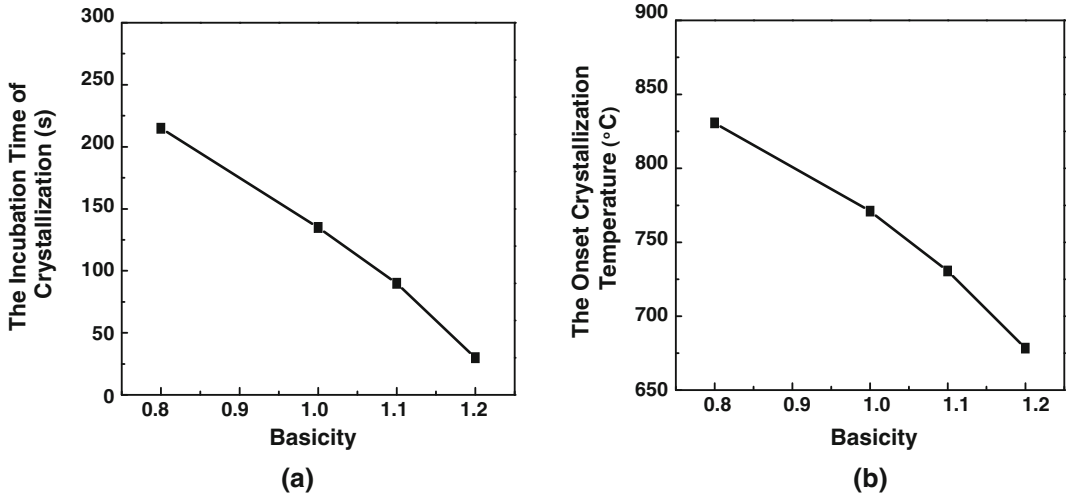

Fig. 10—Relationship between basicity and: (*a*) the incubation time of crystallization and (*b*) the onset crystallization temperature.

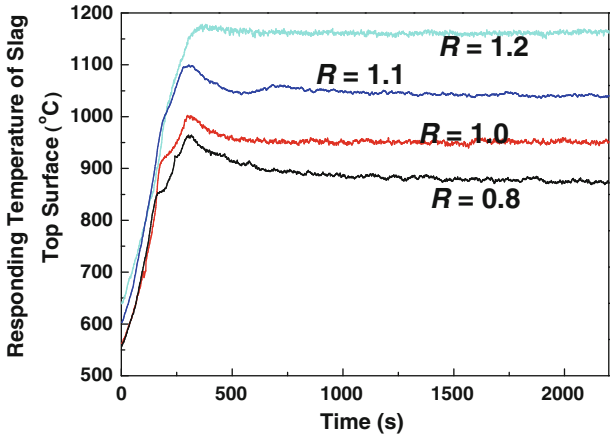

Fig. 11—The measured disks' top surface temperatures for mold fluxes with different basicities.

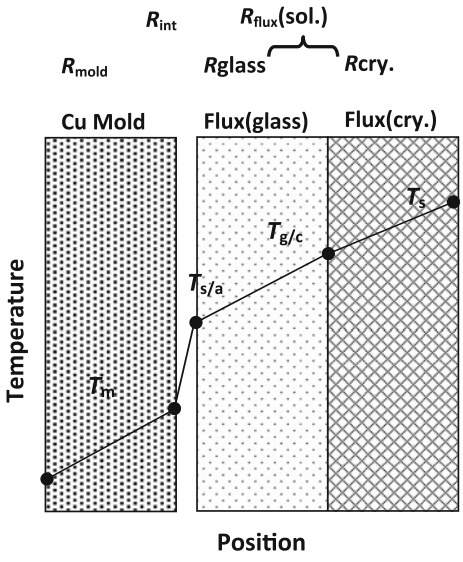

Fig. 12—Schematic temperature distribution across mold flux film consisted of crystalline and glassy layers.

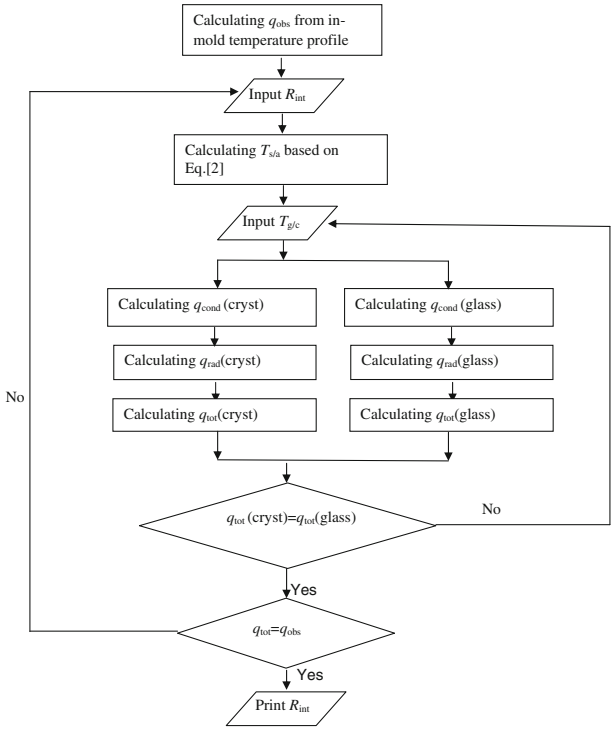

Fig. 13—The flow chart for calculating R_{int}.

Consequently, the total heat fluxes in the crystalline and glassy layer (q_{tot}(crystalline) and q_{tot}(glass)) can be expressed by Eqs. [7] and [8], respectively.

$$q_{tot}(\text{crystalline}) = q_{conduction}(\text{crystalline}) + q_{radiation}(\text{crystalline}) \quad [7]$$

$$q_{tot}(\text{glass}) = q_{conduction}(\text{glass}) + q_{radiation}(\text{glass}) \quad [8]$$

For the steady-state conditions,

$$q_{tot}(\text{crystalline}) = q_{tot}(\text{glass}) \quad [9]$$

Table II. Parameters for Interfacial Thermal Resistance (R_{int}) Calculations

	T_s [K (°C)]	$T_{g/c}$ [K (°C)]	T_m [K (°C)]	$d_{crystalline}$ (mm)	d_{glassy} (mm)
Flux 1 (R = 0.8)	1148 (875)	1103 (830)	376.2 (103.2)	2.30	1.00
Flux 2 (R = 1.0)	1225 (952)	1044 (771)	374.6 (101.6)	2.78	0.52
Flux 3 (R = 1.1)	1313 (1040)	1003 (730)	373 (100)	3.02	0.28
Flux 4 (R = 1.2)	1437 (1164)	951 (678)	364.1 (91.1)	3.30	0

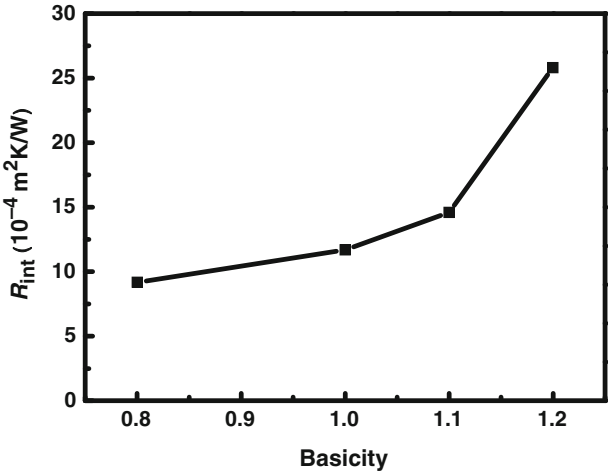

Fig. 14—Calculated interfacial thermal resistances for mold fluxes with various basicities.

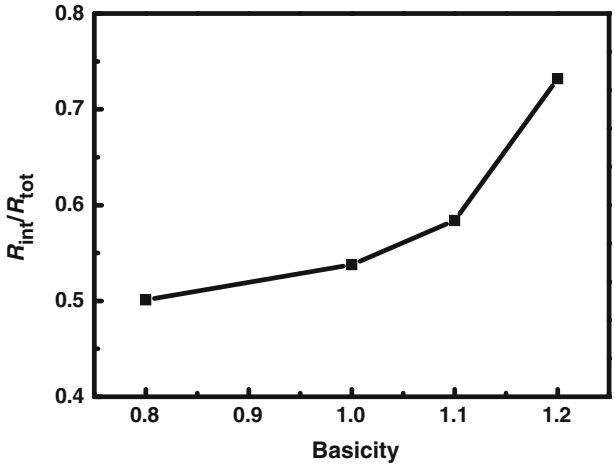

Fig. 16—The ratio of interfacial thermal resistances to total thermal resistances for different mold fluxes.

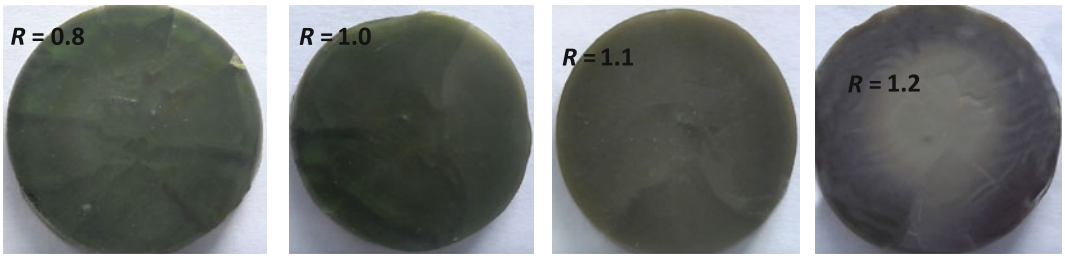

Fig. 15—The bottom surface views of the slag disks with different basicity.

Therefore, the interfacial thermal resistance R_{int} could be computed through Eqs. [8] and [9] as the flow chart shown in Figure 13, where the parameters used for the calculation are shown in Table II. The values of R_{int} were then calculated and shown in Figure 14.

As shown in Figure 14, the steady-state R_{int} increases from 9.2 to 14.6×10^{-4} and then jumps to 25.8×10^{-4} m^2K/W, with the increase of basicity, which indicated that the mold flux crystallization does enhance the interfacial thermal resistance between the copper mold and solid flux. The thicker the crystalline layer, the larger the R_{int} would be. The result was consistent with other researchers' observations,[13,15,34] and the jump of R_{int} may be caused by the complete crystallization of the slag disk when the basicity of slag changes to 1.2.

Figure 15 shows the bottom views of mold disks with various basicities. No wrinkles are apparent at the surface for the slags of R = 0.8, R = 1.0, and R = 1.1. However, the surface of the R = 1.2 disk turns to be rough, and many ripples appear at the bottom surface because of the full crystallization. This rough surface might cause the jump of R_{int} based on Tsutsumi's research.[35]

Figure 16 gives the ratio of the interface resistance R_{int} to the total thermal resistance R_{tot}, where R_{tot} was determined through Eq. [10].

$$R_{tot} = \frac{(T_s - T_m)}{q_{tot}} = R_{slag} + R_{int} \qquad [10]$$

As shown in Figure 16, the ratio varies from 0.501 to 0.732 when the basicity of mold fluxes increases from 0.8 to 1.2, which suggested that the R_{int} is the dominant factor that affects the heat transfer between strand and copper mold. This result was consistent with Cho's report that the ratio of R_{int} to total thermal resistance was approximately 50 pct to 60 pct for different mold fluxes.

IV. CONCLUSIONS

The effect of basicity-introduced mold flux crystallization on the radiative heat transfer and slag/mold interfacial thermal resistance was studied in this article. Several important conclusions were made as follows:

1. Basicity enhances the mold flux crystallization as the solid mold fluxes with a higher basicity would be crystallized when they were subjected to same thermal radiation, and a more thermal radiation would be scattered through the crystals boundary and defects, which resulted in a greater radiation reduction. The measured heat flux passing through the copper mold decreases with the increase of mold flux basicity. The steady-state heat-transfer rate changed from 413 KW/m^2 to 317 KW/m^2 when the basicity was increased from 0.8 to 1.2.
2. The observed incubation time prior to the mold flux crystallization was shorter with the increase of basicity, and the measured onset crystallization temperature also decreased with the addition of basicity. It indicated that CaO, which is an alkali oxide, acts on the silicate network as a network modifier and could enhance the crystallization of mold flux by reducing the glass transition time and the onset crystallization temperature.
3. The study of interfacial thermal resistance between the copper mold and mold flux indicated that the interfacial thermal resistance became larger when the basicity increased, as the subsequent crystallization of mold flux would lead to a greater mold flux contraction and resulted in a rougher bottom surface, which gave rise to the enlargement of interfacial thermal resistance. The ratio of the interfacial thermal resistance to the total thermal resistance showed that the interfacial thermal resistance played a dominant role in the heat transfer in the mold.
4. With the increase of basicity, the subsequent crystallization of mold flux would introduce a higher slag thermal resistance, which in turn would increase the slag top surface temperature at the steady state.

REFERENCES

1. K.C. Mills, A.B. Fox, Z. Li, and R.P. Thackray: *Ironmaking Steelmaking*, 2005, vol. 32 (1), pp. 26–34.
2. Y. Meng and B.G. Thomas: *ISIJ Int*., 2006, vol. 46 (5), pp. 660–69.
3. W. Wang and A.W. Cramb: *ISIJ Int*., 2005, vol. 45 (12), pp. 1864–70.
4. J.F. Holzhauser, K.H. Spitzer, and K. Schwerdtfeger: *Steel Res*., 1999, vol. 70 (7), pp. 252–58.
5. J.F. Holzhauser, K.H. Spitzer, and K. Schwerdtfeger: *Steel Res*., 1999, vol. 70 (10), pp. 430–36.
6. W. Wang, L.J. Zhou, and K.Z. Gu: *Met. Mater. Int*., 2010, vol. 16 (6), pp. 913–20.
7. J.W. Cho, T. Emi, H. Shibata, and M. Suzuki: *ISIJ Int*., 1998, vol. 38 (3), pp. 268–75.
8. K.C. Mills and A.B. Fox: *ISIJ Int*., 2003, vol. 43 (10), pp. 1479–86.
9. M. Hanao and M. Kawanoto: *ISIJ Int*., 2008, vol. 48 (2), pp. 180–85.
10. H. Matsuda, K. Saruhashi, J. Abu, H. Takada, H. Yasunaka, and S. Koyama: *CAMP-ISIJ*, 1992, vol. 5 (1), pp. 207–13.
11. Y. Meng and B.G. Thomas: *Metall. Mater. Trans. B*, 2003, vol. 34B, pp. 707–13.
12. J. Sengupta, H. Shin, B.G. Thomas, and S.-H. Kim: *Acta Mater*., 2006, vol. 54 (6), pp. 1165–73.
13. A. Yamauchi, K. Sorimachi, T. Sakuraya, and T. Fujii: *ISIJ Int*., 1993, vol. 33 (1), pp. 140–47.
14. M. Susa, A. Kushimoto, H. Toyota, M. Hayashi, R. Endo, and Y. Kobayashi: *ISIJ Int*., 2009, vol. 49 (11), pp. 1722–29.
15. K. Watanade, M. Suzuki, K. Murakami, H. Kondo, A. Miyamoto, and T. Shiomi: *Tetsu-to-Hagané*, 1997, vol. 83 (2), pp. 115–20.
16. K. Tsutsumi, T. Nagasaka, and M. Hino: *ISIJ Int*., 1999, vol. 39 (11), pp. 1150–59.
17. H. Mizuno, H. Esaka, K. Shinozuka, and M. Tamura: *ISIJ Int*., 2008, vol. 48 (3), pp. 277–85.
18. M. Hanao, M. Kawanoto, M. Hara, T. Murakami, H. Kikuchi, and K. Hanazaki: *Tetsu-to-Hagané*, 2002, vol. 88 (1), pp. 23–28.
19. H. Nakada, M. Suza, Y. Seko, M. Hayashi, and K. Nagata: *ISIJ Int*., 2008, vol. 48 (4), pp. 446–53.
20. J.W. Cho, H. Shibata, T. Emi, and M. Suzuki: *ISIJ Int*., 1998, vol. 38 (5), pp. 440–46.
21. B.G. Thomas, B. Ho, and G. Li: *Alex Mclean Symposium Proc*, Iron and Steel Society, Warrendale, PA, 1988, pp. 177–93.
22. Z. Li, R. Thackray, and K.C. Mills: *VII Int. Conf. on Molten Slags, Fluxes and Slats*, The South African Institute of Mining and Metallurgy, Johannesburg, South Africa, 2004, pp. 813–20.
23. M. Persson, M. Gornerup, and S. Seetharaman: *ISIJ Int*., 2007, vol. 47 (10), pp. 1533–40.
24. K.C. Mills: *ISIJ Int*., 1993, vol. 33 (1), pp. 148–55.
25. K. Prapakorn: Ph.D. Thesis, Carnegie Mellon University, Pittsburgh, PA, 2003.
26. W. Wang: Ph.D. Thesis, Carnegie Mellon University, Pittsburgh, PA, 2007, pp. 107–20.
27. L. Zhou, W. Wang, F. Ma, J. Li, J. Wei, H. Matsuura, and F. Tsukihashi: *Metall. Mater. Trans. B*, 2011, DOI: 10.1007/s11663-011-9591-5, in press.
28. M. Hayashi, T. Watanabe, H. Nakada, and K. Nagata: *ISIJ Int*., 2006, vol. 46 (12), pp. 1805–09.
29. T. Watanabe, H. Hashimoto, M. Hayashi, and K. Nagata: *ISIJ Int*., 2008, vol. 48 (7), pp. 925–33.
30. W. Wang, K. Gu, L. Zhou, F. Ma, I. Sohn, D.J. Min, H. Matsuura, and F. Tsukihashiet: *ISIJ Inter*., 2011, vol. 51 (11), pp. 1838–45.
31. S. Ozawa, M. Susa, T. Goto, R. Endo, and K.C. Mills: *ISIJ Int*., 2006, vol. 46 (3), pp. 413–19.
32. Y. Shiraishi: *Handbook of Physico-Chemical Properties at High Temperature*, ISIJ International, Tokyo, Japan, 1988, ch. 10.
33. W. Wang and A.W. Cramb: *AIST Trans*., 2008, vol. 5, pp. 155–60.
34. K. Tsutumi, T. Nagasaka, and M. Hino: *ISIJ Int*., 1999, vol. 39 (11), pp. 1150–59.
35. J.W. Cho, T. Emi, H. Shibata, and M. Suzuki: *ISIJ Int*., 1998, vol. 38 (8), pp. 834–42.